

Electronic Supplementary Information

Binding of human serum albumin to PEGylated liposomes: insights into binding numbers and dynamics by fluorescence correlation spectroscopy

Kasper Kristensen,^{a,c} Andrew J. Urquhart,^{a,c} Esben Thormann,^{b,c} and Thomas L. Andresen^{a,c}

^aDepartment of Micro- and Nanotechnology, DTU Nanotech, Technical University of Denmark, 2800 Kongens Lyngby, Denmark, ^bDepartment of Chemistry, DTU Chemistry, Technical University of Denmark, 2800 Kongens Lyngby, Denmark, ^cCenter for Nanomedicine and Theranostics, Technical University of Denmark, 2800 Kongens Lyngby, Denmark

SEC purification of Alexa Fluor 488-labeled HSA after labeling reaction

In the main paper, it was described how the Alexa Fluor 488-labeled HSA was purified by SEC after the labeling reaction. Fig. S1 shows an example of a chromatogram of such an SEC run. Two peaks were observed in the chromatogram, corresponding to labeled protein and unreacted dye, respectively. The two peaks were clearly separated. Of relevance, the dye itself not only absorbed light at 494 nm but also at 280 nm. This fact was taken into account when quantifying the HSA content of the first peak in the chromatogram (see Eq. 1 in the main paper).

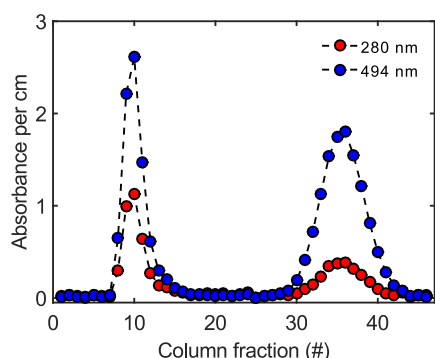


Figure S1: Typical chromatogram of an SEC run conducted to purify Alexa Fluor 488-labeled HSA after the labeling reaction.

Basic characterization of liposomes

In the main paper, it was described how the zeta potentials and sizes of the liposomes were measured by phase analysis light scattering and dynamic light scattering, respectively. The results of these measurements are shown

in Fig. S2. Fig. S2A shows that the zeta potentials of the liposomes were slightly negative. In addition, there was a tendency that the zeta potentials depended on the lipid composition of the liposomes; specifically, liposomes with high content of PEGylated lipid had a slightly lower zeta potential than liposomes with low content of PEGylated lipid. Fig. S2B shows that the hydrodynamic diameters of the liposomes were ~110-130 nm, largely independent of the lipid composition. Of importance, similar hydrodynamic diameters were measured in FCS experiments on fluorescently labeled liposomes (data not shown), indicating that there was no significant bias between the liposome size estimates provided by dynamic light scattering and FCS.

Expanded FCS theory

In the main paper, we presented a simple two-component mathematical framework for using FCS for studying protein binding to liposomes. The following section provides a more elaborate discussion of this framework to allow for a more complete interpretation of our FCS results.

According to Eq. 4 in the main paper, the amplitude of the autocorrelation curve associated with the free proteins, A_f , is given by

$$A_f = \frac{B_f^2 N_f}{F_t^2} \quad (\text{S1})$$

where N_f is the apparent mean number of free proteins in the detection volume and B_f is the apparent brightness of the free proteins. Likewise, the amplitude of the autocorrelation curve associated with the bound protein, A_s , is given by

$$A_s = \frac{B_s^2 N_s}{F_t^2} \quad (\text{S2})$$

where N_s is the apparent mean number of liposomes with bound protein in the detection volume and B_s is the apparent brightness of the liposomes with bound protein.

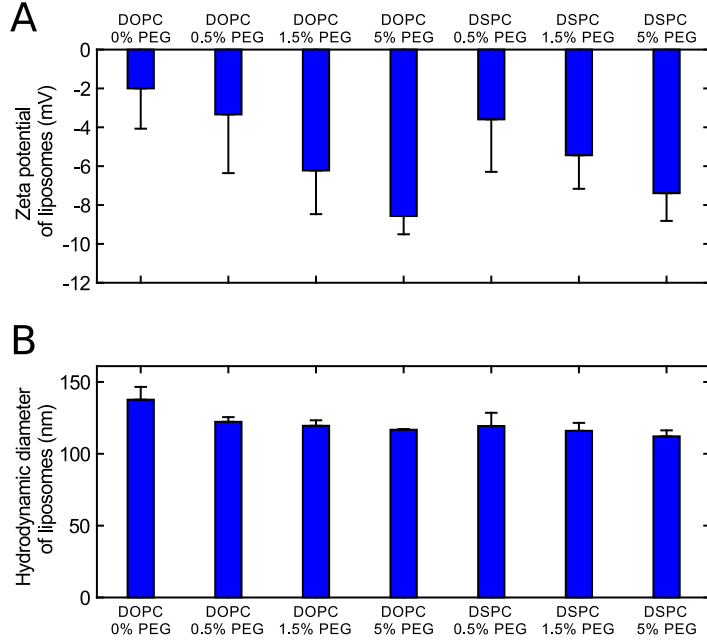


Figure S2: Basic characterization of the liposomes. (A) Zeta potentials of the liposomes as determined by phase analysis light scattering. (B) Hydrodynamic diameters of the liposomes as determined by dynamic light scattering. In both panels, the error bars represent the experimental standard deviations.

The total photon count rate, F_t , is given by

$$F_t = B_f N_f + B_s N_s. \quad (S3)$$

The mole fraction of protein bound to the liposomes, f_b , is given by

$$f_b = \frac{N_b}{N_t} \quad (S4)$$

where N_b is the apparent mean number of liposome-bound proteins in the detection volume and N_t is the apparent total mean number of proteins in the detection volume, given by

$$N_t = N_f + N_b. \quad (S5)$$

The apparent number of proteins per liposome, b , is given by

$$b = \frac{N_b}{N_s}. \quad (S6)$$

If the apparent brightness of free proteins and liposome-bound proteins is the same (which is the case for the Alexa Fluor 488-labeled HSA), then b can also be written as

$$b = \frac{B_s}{B_f}. \quad (S7)$$

In the limit in which no liposomes have bound more than one protein, $b = 1$. In case that some liposomes have bound more than one protein, $b > 1$.

One of the output parameters of our FCS experiments was the fractional amplitude of the autocorrelation curve

associated bound protein, y_s , given by Eq. 7 in the main paper. By use of the Eqs. S1, S2, S6, and S7, Eq. 7 can be rewritten to

$$y_s = \frac{b N_b}{N_f + b N_b}. \quad (S8)$$

In case that no liposomes have bound more than one protein ($b = 1$), then $y_s = f_b$. In case that some liposomes have bound more than one protein ($b > 1$), then $y_s > f_b$.

Another output parameter of our FCS experiments, which we did not consider in the main paper, was the total amplitude of the autocorrelation curve, A_t , given by

$$A_t = A_f + A_s. \quad (S9)$$

By use of Eqs. S1-S3 and S5-S7, Eq. S9 can be rewritten to

$$A_t = \frac{N_f + b N_b}{N_t^2}. \quad (S10)$$

In case that no liposomes have bound more than one protein ($b = 1$), then $A_t = N_t^{-1}$. In case that some liposomes have bound more than protein ($b > 1$), then $A_t > N_t^{-1}$. Thus, in our experiments where the total concentration of fluorescently labeled protein was constant, an increase in A_t indicated that some liposomes had bound more than one labeled protein.

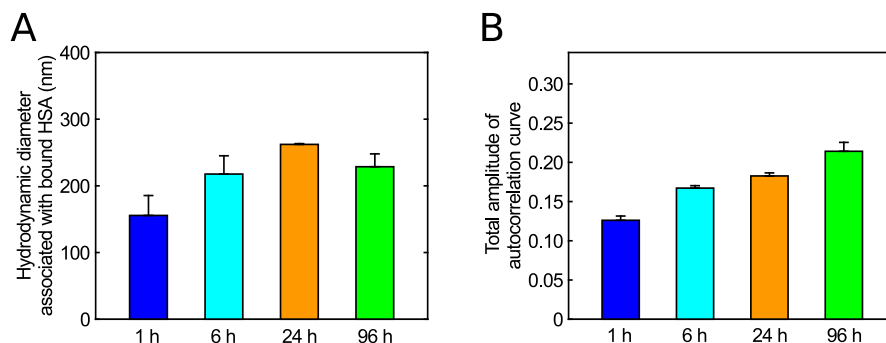


Figure S3: Supporting results to Fig. 2 in the main paper. (A) Hydrodynamic diameters associated with bound HSA as a function of incubation time. (B) Total amplitudes of autocorrelation curves as a function of incubation time. In both panels, the error bars represent the experimental standard deviations.

Supporting results to the FCS results presented in the main paper

Figs. 2-4 in the main paper showed our most important FCS results. Figs. S3-S5 show some additional supporting FCS results to substantiate the interpretation and understanding of the results in Figs 2-4.

Supporting results to Fig. 2

Fig. S3 shows some supporting results to Fig. 2. Specifically, Fig. S3A shows how the hydrodynamic diameter associated with bound HSA depended on the incubation time. The diameter of 220 ± 40 nm stated in the main paper was calculated by averaging the diameters in Fig. S3A across the investigated incubation times. Fig. S3B shows how the total amplitude of the autocorrelation curves depended on the incubation time. The total amplitude increased as a function of HSA binding to the liposomes (compare Fig. S3B to Fig. 2C). According to Eq. S10, this indicates that some liposomes—or maybe more precisely liposome aggregates—bound more than one HSA molecule. According to Eq. S8, this in turn indicates that the fractional amplitudes presented in Fig. 2C are higher than the real mole fractions of HSA that bound to the liposomes.

Supporting results to Fig. 3

Fig. S4 shows some supporting results to Fig. 3 for those of the experiments done with the DSPC-based PEGylated liposomes. Specifically, Fig. S4A,B shows how the hydrodynamic diameter associated with bound HSA depended on the HSA concentration and incubation time. The diameters presented in Fig. 3C were calculated by averaging the diameters in Fig. S4A,B across the investigated HSA concentrations and incubation times. Fig. S4C,D shows how the total amplitude of the autocorrelation curves depended on the HSA concentration and incu-

bation time. In the experiments with the DSPC/DSPE-PEG2k (99.5:0.5) and DSPC/DSPE-PEG2k (98.5:1.5) liposomes, the total amplitude increased as a function of HSA binding to the liposomes (compare Fig. S4C,D to Figure 3A,B). As mentioned above, this indicates that the fractional amplitudes presented in Fig. 3A,B are higher than the real mole fractions of HSA bound to these types of liposomes. In contrast, in the experiments with the DSPC/DSPE-PEG2k (95:5) liposomes, the total amplitude of the autocorrelation curves associated with bound HSA did not change as a function of HSA binding, indicating that the fractional amplitudes presented in Fig. 3A,B are equal to the real mole fractions of HSA that bound to this type of liposomes.

Supporting results to Fig. 4

Fig. S5 shows some supporting results to Fig. 4. Specifically, Fig. S5A shows the hydrodynamic diameters associated with bound HSA and Fig. S5B shows the total amplitudes of the autocorrelation curves. In agreement with the data in Figs. S3 and S4, the total amplitudes increased as a function of HSA binding in the experiments with the DSPC/DSPE-PEG2k (99.5:0.5) and DSPC/DSPE-PEG2k (98.5:1.5) liposomes (compare Fig. S5B to Fig. 4).

Supporting results to the SEC/FCS results presented in the main paper

Example of full SEC elution profile

In the main paper, a set of SEC/FCS experiments were described. As part of the protocol for these experiments, HSA/liposome samples were loaded onto an SEC column. For each sample, 24 column fractions were then collected. In a few cases, all of these 24 column fractions were investigated by FCS. Specifically, volumes of all of the 24

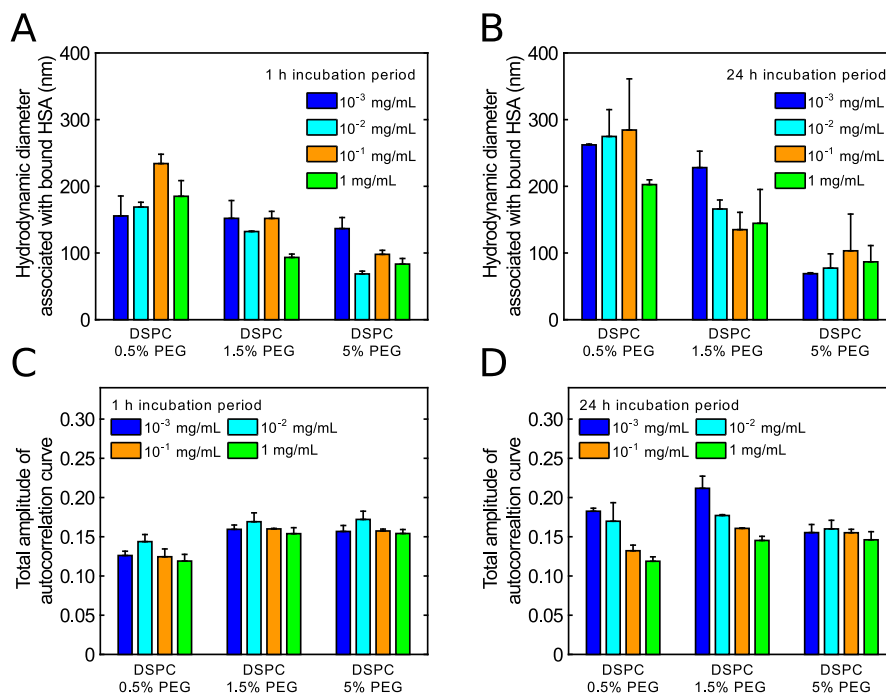


Figure S4: Supporting results to Fig. 3 in the main paper. (A,B) Hydrodynamic diameters associated with bound HSA as a function of HSA concentration after 1 h incubation (A) or 24 h incubation (B). (C,D) Total amplitudes of autocorrelation curves as a function of HSA concentration after 1 h incubation (C) or 24 h incubation (D). In all panels, the error bars represent the experimental standard deviations.

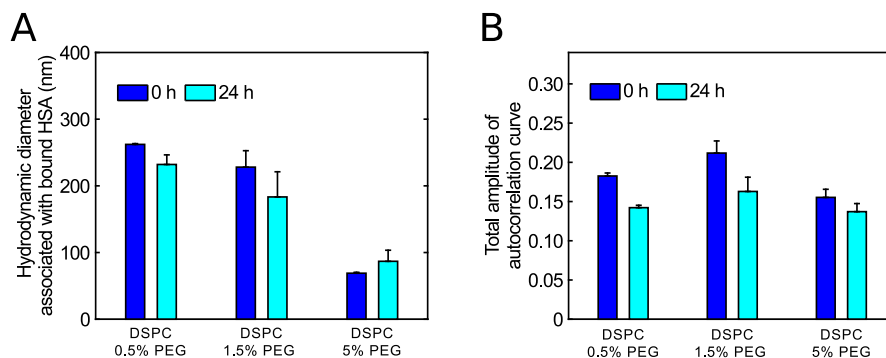


Figure S5: Supporting results to Fig. 4 in the main paper. (A) Hydrodynamic diameters associated with bound HSA. (B) Total amplitudes of autocorrelation curves. The "0 h" bars show the results at the time of unlabeled HSA addition. The "24 h" bars show the results 24 h after the addition of unlabeled HSA. In both panels, the error bars represent the experimental standard deviations.

column fractions were transferred to pre-coated eight-well chambered coverslips. Each of the column fractions were then examined by FCS using an acquisition time of 1 min per column fraction. All of the 24 acquired autocorrelation curves were subsequently fitted by use of a single-component model (Eq. 3 in the main paper). Fig.

S6 shows the results of such an experiment, conducted using a sample of 0.1 mg/mL labeled HSA and 10 mM DSPC/DSPE-PEG2k (99.5:0.5) liposomes (concentration in terms of lipid) incubated for 24 h at 37 °C prior to SEC. Specifically, Fig. S6A shows the photon count rates of the column fractions, demonstrating that HSA eluted

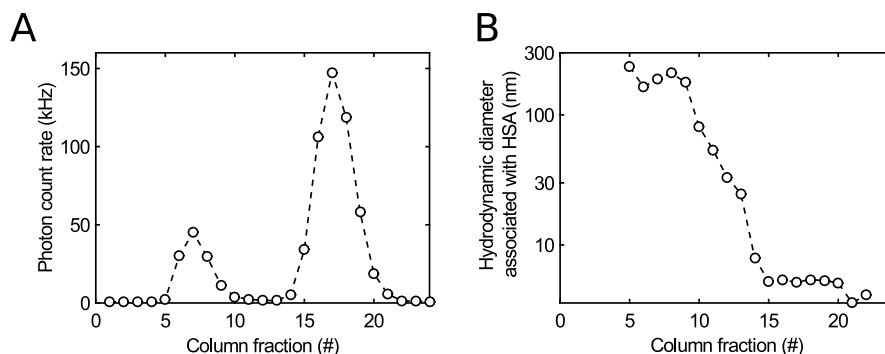


Figure S6: Example of full SEC elution profile underlying an SEC/FCS experiment. A sample containing 0.1 mg/mL labeled HSA and DSPC/DSPE-PEG2k (99.5:0.5) liposomes (10 mM lipid) was prepared. The sample was incubated for 24 h at 37 °C. After incubation, the sample was run on an SEC column. Twenty-four column fractions were collected and subsequently investigated by FCS. (A) Total photon count rates of the column fractions. (B) Hydrodynamic diameters associated with HSA in the column fractions.

in two distinct peaks. Fig. S6B shows the hydrodynamic diameters associated with HSA in the column fractions. The hydrodynamic diameters associated with HSA in the column fractions of the first peak were ~200 nm, implying that HSA eluting in this peak was associated with liposome aggregates. The hydrodynamic diameters associated with HSA in the column fractions of the second peak were ~5.6 nm, showing that HSA eluting in this peak was free in solution.

Supporting results to Fig. 5

As described in the main paper, the 24 column fractions of each SEC run were generally pooled into two samples containing (i) the HSA that had remained bound to the liposomes during the SEC separation step and (ii) free HSA, respectively. These two samples were then investigated by FCS. Fig. 5 in the main paper showed the most important results of these experiments. Fig. S7 shows some additional supporting results to Fig. 5, obtained by fitting the autocorrelation curves of the SEC samples containing the HSA that had remained bound to the liposomes during the SEC separation step with a two-component model. Specifically, Fig. S7A,B shows how the fractional amplitudes of the autocorrelation curves associated with bound HSA depended on the HSA concentration and incubation time. The fractional amplitudes associated with bound HSA were generally close to 1, indicating close to complete HSA binding to the liposomes. However, in some cases, the fractional amplitudes of the autocorrelation curves were slightly lower, below ~0.8, indicating that some HSA in these cases dissociated from the liposomes after the SEC run. Fig. S7C,D shows how the hydrodynamic diameters associated with bound HSA depended on the HSA concentration and incubation time. The diameters presented in Fig. 5C were calculated by averaging the diameters in Fig. S7C,D across the investigated HSA concentrations and incubation times.

Binding of unlabeled HSA to liposomes

The overall aim of these experiments was to get an indication of whether fluorescent labeling of HSA with Alexa Fluor 488 influenced the liposome-binding properties of the protein. Chloroform, methanol, and sodium dodecyl sulfate (SDS) used for these experiments were purchased from Sigma-Aldrich. Micro-BCA protein assay kit was purchased from Thermo Fisher Scientific.

Method

Samples containing 1 mg/mL unlabeled HSA and 10 mM of one of the different types of DSPC-based PEGylated liposomes (concentration in terms of lipid) were prepared in Protein LoBind tubes. The samples were incubated for 24 h at 37 °C. Then, 500 µL of each of the samples was loaded onto a Sepharose CL-4B column and eluted with PBS at a flow rate of ~1 mL/min. After 5 min waiting, the eluent was collected in Protein LoBind tubes in 1 min column fractions. The column fractions with liposomes could be recognized because these fractions appeared opaque. Equal volumes of the opaque column fractions were pooled into one common Protein LoBind tube. By this approach, from each sample run on the SEC column, a new sample containing the HSA that remained bound to the liposomes during the SEC separation step was obtained.

We next wanted to estimate the HSA concentration in the collected SEC samples by use of a micro-BCA assay. For this purpose, we first transferred 100 µL of each of the SEC samples to Protein LoBind tubes. We also prepared 100 µL standard samples with HSA mass concentrations between 0 and 100 µg/mL in PBS in Protein LoBind tubes. Because lipids may interfere with the micro-BCA assay, all samples were then delipidated by use of a protocol similar to a previously described protocol:^{S1} 400 µL methanol was added to all samples. The samples were

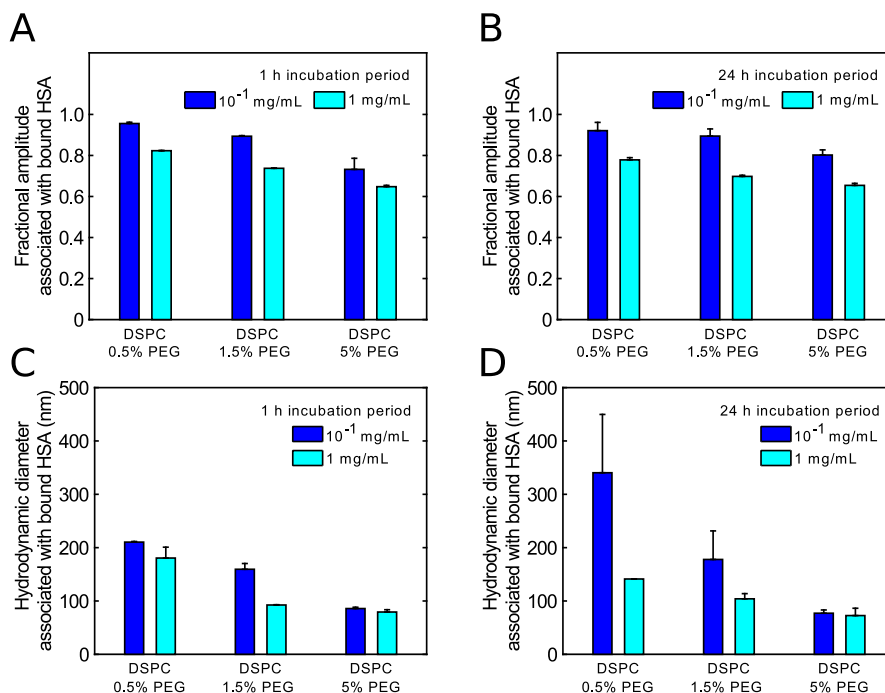


Figure S7: Supporting results to Fig. 5 in the main paper determined from the autocorrelation curves of the SEC samples containing the HSA that had remained bound to the liposomes during the SEC separation step. (A,B) Fractional amplitudes of the autocorrelation curves associated with bound HSA as a function of HSA concentration after 1 h incubation (A) or 24 h incubation (B) prior to SEC. (C,D) Hydrodynamic diameters associated with bound HSA as a function of HSA concentration after 1 h incubation (C) or 24 h incubation (D) prior to SEC. In all panels, the error bars represent the experimental standard deviations.

vortexed and briefly spun down using a Spectrafuge mini laboratory centrifuge (Labnet International, Edison, NJ). Then, 200 μ L chloroform was added to all samples, and the samples were again vortexed and spun down using the Spectrafuge mini laboratory centrifuge. Subsequently, 300 μ L Milli-Q water was added to all samples, creating phase separated mixtures. The samples were vortexed and, next, centrifuged for 4 min at 9000g using a MiniSpin microcentrifuge (Eppendorf). Then, 700 μ L of the upper phase was carefully removed by pipette from all samples. After that, 300 μ L methanol was added to all samples. The samples were vortexed and centrifuged for 4 min at 9000g using the MiniSpin microcentrifuge to pellet the protein. The supernatant was then decanted from all samples. Samples were briefly spun down using the Spectrafuge mini laboratory centrifuge. Residual supernatant was removed by placing the tubes under a gentle flow of nitrogen. The tubes then contained a dry protein pellet. The pellets were resuspended using 145 μ L 5% SDS solution. All samples were vigorously vortexed to completely suspend the protein. Next, 125 μ L of all samples were transferred to new Protein LoBind tubes.

The delipidated samples were then ready for investigation by the micro-BCA assay. Thus, 125 μ L micro-BCA working reagent was added to all samples. The samples

were vortexed and then placed for 1 h in a 60 $^{\circ}$ C water bath. After that, the samples were allowed to cool to room temperature for a few minutes. Subsequently, 220 μ L of each sample was transferred to a 96-well microtiter plate to measure the absorbance at 570 nm by use of a Victor³ 1420 Multilabel Counter (PerkinElmer, Waltham, MA). An absorbance-mass concentration standard curve was prepared by use of the HSA standard samples. Finally, the HSA mass concentrations of the SEC samples could be estimated by comparing their absorbances to the standard curve.

From the protein concentration of a given SEC sample, the mole fraction of HSA that had remained bound to the liposomes during the SEC run, f_b , was calculated:

$$f_b = \frac{n_s V_s c_s}{m_t} \quad (\text{S11})$$

where c_s is the HSA mass concentration of the SEC sample, n_s is the number of column fractions used to prepare the SEC sample, V_s is the volume of the column fractions used to prepare the SEC sample, and $m_t = 0.5$ mg is the total mass of HSA added to the SEC column. For completeness, it should be mentioned that there were some experimental uncertainty associated with the protein concentrations determined by the above method. To mini-

mize the impact of this uncertainty on the determined values of f_b , we used a constant value of m_t in Eq. S11 instead of measuring m_t from the eluted column fractions in each individual experiment.

Results

Fig. S8 shows the mole fraction of unlabeled HSA bound to the different types of DSPC-based PEGylated liposomes. Of importance, the binding levels of unlabeled HSA were similar to the binding levels of labeled HSA (compare the results in Fig. S8 to the "1 mg/mL" bars in Fig 5B). This implies that the labeling of HSA with Alexa Fluor 488 did not change the affinity of the protein for binding to liposomes, at least for the types of liposomes investigated in the present study.

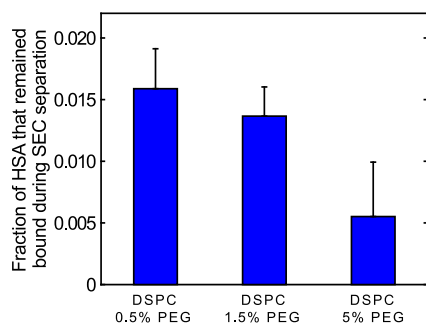


Figure S8: Binding of unlabeled HSA to DSPC-based PEGylated liposome investigated by SEC/micro-BCA method. Samples containing 1 mg/mL unlabeled HSA and one of the different types of DSPC-based PEGylated liposomes (10 mM lipid) were prepared. The samples were incubated for 24 h at 37 °C. Next, the HSA/liposome structures were separated from unbound HSA by SEC. Finally, a micro-BCA assay was used to measure the mole fractions of HSA that remained bound to the liposomes during the SEC step. The error bars represent the experimental standard deviations.

Supporting references

- S1. D. Wessel and U. I. Flügge. *Anal. Biochem.*, 1984, **138**, 141-143.